Methods for Performance Evaluation of Photovoltaic Plants with Reduced Instrumentation

João F. S. de Paula, João L. S. Silva, Marcelo V. de Paula, Gustavo Fraidenraich and Tárcio A. S. Barros

Universidade Estadual de Campinas, Campinas (Brazil)

Abstract

Accurate performance assessment of photovoltaic power plants (PVPPs) typically relies on high-quality in-field measurements, which can be impractical for small-scale systems or arrays with varied orientations. As an alternative, the use of satellite-based datasets (SBDs) combined with physical models (PhM) offers a cost-effective and scalable approach for estimating meteorological conditions and predicting PV performance. This study proposes a reproducible framework for PV system evaluation that integrates open-access SBDs and deterministic PhM within the pvlib-python environment. The framework estimates plane-of-array (POA) irradiance, module temperature, and AC energy yield while minimizing instrumentation requirements to only two irradiance sensors. It includes a systematic method for selecting the most suitable GHI source and decomposition models for POA irradiance estimation. The model chain employs the DIRINT and Erbs models for decomposition, the Perez model for transposition, the Faiman model for PV module temperature, and PVWatts for energy simulation. Validation using six 3.74 MWp single-axis tracking PV plants in southeastern Brazil showed monthly POA irradiation deviations below 3% (except May, 6.5%) and AC energy yield nRMSE between 3.05% and 6.6%, with MAPE from 2.42% to 5.01% and annual bias under 1.2%. The framework demonstrated high accuracy and robustness, providing a practical and sensor-efficient approach for PV performance assessment using open-access data and tools.

Keywords: pvlib, Satellite-Based Database, Performance Ratio, Model Chain, Solarimetric Station, IEC 61724-1:2021

1. Introduction

Reliable meteorological measurements are fundamental for the accurate assessment and monitoring of photovoltaic power plants (PVPPs) (IEC 61724-1, 2021). Among these, plane-of-array (POA) irradiance and module temperature are the most critical parameters, as they directly influence PV energy yield estimation and performance evaluation (De Paula et al., 2024). The precision and temporal resolution of environmental and electrical measurements strongly affect key performance indicators (KPIs), which are essential for reliable system assessment and decision making (Lindig et al., 2024; Sengupta et al., 2024).

The acquisition and maintenance of high-quality sensors remain challenging due to cost and operational complexity (Jahn et al., 2022), particularly for residential-scale systems that dominate the Brazilian distributed generation market (ABSOLAR, 2025; Masson et al., 2024). More complex configurations, such as bifacial modules (Campos et al., 2025), multiple orientations (Sengupta et al., 2024), or partial shading from cloud transients (Wald, 2021), further increase the number of required sensors and system complexity.

Commercial satellite-based datasets (SBDs) such as Solargis (2025) and Meteonorm (2025) provide real-time and historical meteorological data, supporting performance analysis of PV systems. Several studies have benchmarked SBDs under diverse climatic conditions. Riise et al. (2024) evaluated datasets that have high latitudes with significant snow cover found strong agreement for geostationary satellites such as Solargis. Salazar et al. (2020) analyzed SBDs over semi-arid region near the Equator using university on-site data, while Barros et al. (2025) compared datasets across southeastern Brazil using INMET ground measurements. These studies are essential for identifying the most suitable SBD for each region, thereby enhancing the reliability of

10.18086/swc.2025.04.33 Available at http://proceedings.ises.org

feasibility analyses, performance evaluations, and data gap-filling procedures (Sengupta et al., 2024).

Nevertheless, the scarcity of high-resolution in-field solarimetric data, even with initiatives such as SolarStations.org (Jensen, 2025), limits broader validation efforts. When available, high-quality local datasets enable detailed assessments of satellite-derived solar resource data across multiple temporal scales (Dazhi, 2018; Sengupta et al., 2024).

PV performance can also be evaluated through physical model chains that estimate energy yield from meteorological inputs (Mahmoudi et al., 2024; De Medeiros et al., 2025). These typically involve irradiance decomposition and transposition, module temperature estimation, and electrical modeling. The appropriate selection of decomposition and transposition models is critical, as it directly influences prediction accuracy (Sengupta et al., 2024). Although commercial tools such as PVsyst (2025) are widely used for their robustness, their proprietary nature limits flexibility. Conversely, open-access datasets such as PVGIS 5.3 (Joint Research Centre, 2024), NSRDB (NREL, 2025), and NASA POWER (2025), combined with pvlib-python library (Holmgren, 2018), enable transparent and reproducible modeling.

This study proposes a comprehensive framework for PV performance assessment that integrates open-access satellite datasets, physical transposition models, and deterministic energy yield simulations within the pvlib-python environment. The framework is validated using data from six 3.74 MWp monofacial and single axis tracking PV power plants located in southeastern Brazil. The main contributions are: (i) evaluating the accuracy of open-access SBDs and physical models for POA irradiance and energy yield prediction, and (ii) providing a replicable and sensor-efficient framework for PV performance assessment under real operating conditions.

2. Literature Review

Accurate characterization of local meteorological conditions is essential for PV applications, particularly in feasibility studies and performance assessment of PV systems (Sengupta et al., 2024). Meteorological data, such as global horizontal irradiance (GHI) and its components, Direct Normal (DNI) and Diffuse Horizontal (DHI) Irradiances, air temperature, wind speed and others, can be obtained from in-field measurements or SBDs. In-field data, collected with high-quality pyranometers and temperature sensors, are the most accurate and reliable, but their installation and maintenance can be costly or impractical for large-scale systems.

As an alternative, satellite-based datasets offer a practical and cost-effective means of obtaining meteorological data for PV analysis. Although SBDs generally show higher uncertainties compared to ground-based measurements (Salazar et al., 2020), they provide extensive spatial and temporal coverage. To improve their accuracy, bias correction and statistical downscaling techniques are often applied for site adaptation (Sengupta et al., 2024; Yang et al., 2024). For PV applications, the most relevant parameters derived from SBDs are the GHI and DNI, which are essential for estimating solar resource potential and energy yield (Larrañeta et al., 2019; Sengupta et al., 2024).

Among the most used open-access databases are PVGIS 5.3 (Joint Research Centre, 2024), the National Solar Radiation Database (NSRDB) (NREL, 2025), and NASA POWER (2025). The NSRDB is generated using the Physical Solar Model version 4 (PSM v4), an advanced radiative transfer algorithm that provides hourly global estimates of GHI, DNI, and DHI. PSM v4 introduces several improvements, including a physics-guided neural network (PHYGNN) for cloud property correction and gap filling, enhanced surface albedo estimation using MODIS and IMS data, and integration of the FARMS-DNI model for more accurate direct irradiance under all-sky conditions (Sengupta et al., 2025). It also refines solar position calculations, expands satellite coverage through the inclusion of GOES, Meteosat, and Himawari constellations, and improves data consistency across regions. Validation against ground-based networks such as SURFRAD and SRRL showed reduced uncertainty, typically below 5% for GHI and 8% for DNI, with a 25% improvement in DNI accuracy compared to previous versions (Sengupta et al., 2025).

The NASA POWER dataset, derived from the MERRA-2 reanalysis and the Goddard Earth Observing System (GEOS) assimilation models, provides global meteorological parameters such as temperature, wind speed, and solar irradiance, with a spatial resolution of 0.5° (NASA POWER, 2025). In the study by Barros et al. (2025), NASA POWER achieved an nRMSE of 28.3% compared to INMET measurements across southeastern Brazil, ranking as the second-best performing SBD among those analyzed. PVGIS 5.3 also demonstrated satisfactory results for solar resource estimation from the SARAH2, SARAH3, and ERA5 satellites, integrating empirical and semi-empirical models to provide POA irradiance and energy yield estimations for different PV configurations (Joint Research Centre, 2024).

In summary, open-access satellite-based datasets, combined with improved physical modeling frameworks such as PSM v4, have advanced the capability to assess PV performance in regions with limited ground measurements. When properly validated and bias-corrected, these datasets provide a reliable and scalable solution for feasibility studies, long-term energy yield prediction, and performance assessment of PV systems under diverse climatic conditions.

2.1. PV System Energy Yield Modeling through Model Chain Method

PV energy yield estimation is commonly performed using the model chain approach, which consists of a sequence of physical and empirical models describing how meteorological variables influence the energy conversion process of PV systems (Mahmoudi et al., 2024; De Medeiros et al., 2025). The process begins with the estimation of solar irradiance components. From measured or satellite-derived GHI, the DNI and DHI are derived through decomposition models such as Erbs et al. (1982), Disc (Maxwell, 1987), Dirint (Perez et al., 1992), and Boland et al. (2001).

Decomposition models play a key role in determining DNI and DHI from GHI, serving as critical inputs for transposition and performance modeling. The Erbs model (1982) provides an empirical correlation between the diffuse fraction (DHI/GHI) and the clearness index (Kt) through polynomial regressions based on extensive U.S. data, performing best under clear to moderately cloudy conditions. The Disc model (Maxwell, 1987) applies a semi-empirical correction factor to extraterrestrial radiation, incorporating air mass and atmospheric transmittance to improve accuracy under variable sky conditions.

The Dirint model (Perez et al., 1992) enhances this approach by using one-minute GHI data and clear-sky indices, increasing responsiveness to rapid irradiance fluctuations caused by cloud transients. The Boland model (2001) further refines diffuse fraction estimation using a logistic function that incorporates both clearness index and solar elevation angle, improving continuity between sky conditions and performance in humid and tropical climates. Together, these models represent a progression from simple empirical correlations to hybrid formulations with enhanced temporal and climatic adaptability.

Using the derived components, anisotropic transposition models such as Perez et al. (1990) convert irradiance from the horizontal to the POA, within its direct (DIR), diffuse (DIF), and reflected (REF) components, improving mainly the representation of the DIF component compared to isotropic formulations (Liu and Jordan, 1960). Subsequent optical corrections account for incidence angle modifier (IAM) effects (Souka and Safwat, 1966), which depend on the angle of incidence (AOI) of the direct POA irradiance, as well as for losses due to soiling, shading, and reflection. These corrections yield the effective POA irradiance incident on the PV surface, which serves as the foundation for subsequent temperature and electrical modeling stages in the energy yield simulation process.

The cell operating temperature is then estimated from ambient temperature and wind speed using empirical thermal models, such as the Faiman (2008), which relates module temperature to irradiance and convective cooling conditions. With the effective POA irradiance, cell temperature, and PV module parameters, the PVWatts model (Dobos, 2014) is used to estimate the DC power output of the PV array. The DC energy yield, P_{sim}, can be calculated using Eq. 1:

$$P_{sim} = Po * \frac{G}{Go} * \left(1 + \varphi * (T - 25)\right) * Ltotal \qquad \text{(eq. 1)}$$

where P_0 is the nominal PV system capacity (the product of the module rated power at standard test conditions, P_{mp}, and the total number of modules), G is the POA irradiation (Wh/m²), $G_0 = 1000$ W/m^2 is the irradiance under standard test conditions, φ is the temperature coefficient of P_{mp}, and T is the operating cell temperature. System losses are represented by L_{total}, which consolidates the effects of multiple loss mechanisms such as mismatch, unavailability, and partial shading. The combined impact of these losses is expressed as (Eq. 2):

$$Ltotal(\%) = 100 * [\, 1 - \prod_i (1 - \frac{Li}{100})] \qquad \text{(eq. 2)}$$

where L_i represents the percentage loss contribution of each individual source. Multiplying Eq. (1) and (2) yields a more realistic estimation of the modeled DC energy yield. Finally, the DC output is converted to AC power through inverter models (Jensen et al., 2023; Holmgren et al., 2018), accounting for inverter efficiency, clipping, and conversion losses when the generated power exceeds the inverter's rated capacity.

3. Methodology

The present work proposes a framework for accurate PV system energy yield modeling, relying exclusively on satellite-based datasets and a chain of physical models implemented using the pvlib-python library. The framework is structured into three main stages: (1) selection of the meteorological satellite-based database providing the most accurate GHI estimates across hourly, daily, and monthly resolutions; (2) identification of the optimal pair of physical-based decomposition and transposition models, through combinatory analysis, that yield the most accurate predictions of POA irradiance; and (3) comparative analysis between modeled AC energy yield and electrical measurements from the PV power plant to assess system performance. The operational flow of the proposed framework is illustrated in Figure 1.

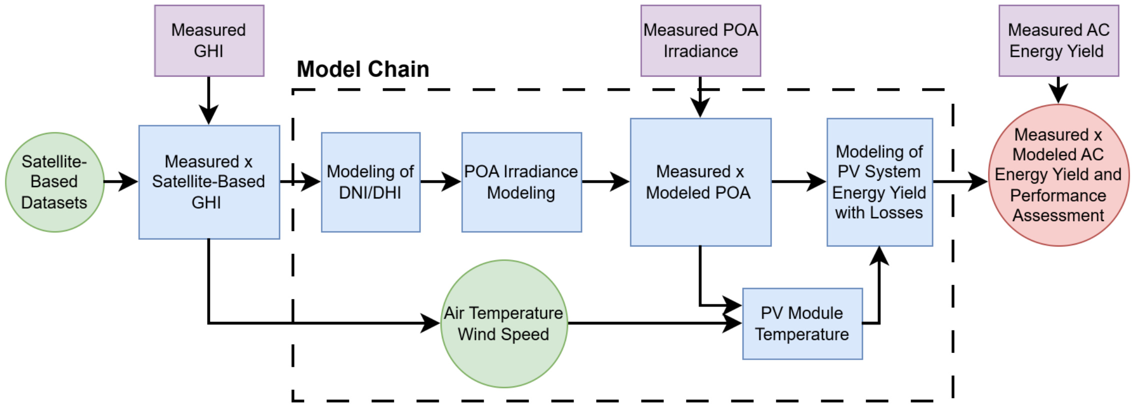

Figure 1: Flowchart of the proposed framework.

3.1. Description of PV Power Plants Characteristics

The proposed framework was validated using in-field electrical and meteorological data from a utility-scale PV power plant. The validation aimed to ensure high accuracy in estimating solar irradiance on both horizontal and POA surfaces, as well as in predicting system energy yield for feasibility studies and operational performance assessments. The reference PV plant, located in southeastern Brazil, comprises six independent PV systems, each rated at 3.74 MWp and configured with single-axis tracking. The arrays use monofacial modules with a $P_{mp} = 330$ Wp and a $\varphi = -0.38\%/°C$.

The facility includes a solarimetric station equipped with three sensors at the central monitoring unit and two additional sensors installed on the PV strings. All instruments comply with the accuracy and classification requirements of IEC 61724-1:2021. Table 1 summarizes the solarimetric instrumentation specified by the equipment adopted in the reference plant and the reduced set of sensors required by the proposed modeling framework. In Table 1, "S" denotes a sensor, while "PhM" represents the physical models integrated within the model chain.

Table 1: Comparative of existent sensors used in the PV power plant of the present work and the sensors required by the proposed framework operation.

Weather Parameters	GHI	DNI	DHI	T_{air}	WS	POA	T_{mod}	Total
In-Field Measurements	S	-	-	S	S	S	S	5
Framework	SBD⁺	SBD/PhM	SBD/PhM	SBD	SBD	PhM⁺	PhM	2

⁺The sensors are required for benchmarking of satellite-based datasets and decomposition and transposition models selection.

As shown in Table 1, the proposed framework seeks to reduce the dependency on multiple sensors: from five to two strategically positioned pyranometers measuring global irradiance on both horizontal and POA surfaces. Besides, it provides two more weather parameters for PV performance analysis. These pyranometers are classified as Class B, following the criteria from ISO 9060 (2018), which, despite presenting higher uncertainty compared to Class A instruments, are considered adequate for the analyses conducted in this study.

The electrical and meteorological data used for validation were collected throughout 2020, corresponding to the first year of operation of the PV power plant. This period was characterized by stable system performance and minimal operational issues, providing a reliable reference for model validation. The solarimetric datasets underwent preliminary quality control procedures and did not present critical data gaps, ensuring no adverse impact on the analyses performed in this work.

3.2. Satellite-Based Databases and Model Chain Composition for PV Energy Yield Modeling

For this study, three free-access SBDs were selected for comparison: NASA POWER, NSRDB (PSMv4), and PVGIS 5.3. Within PVGIS 5.3, the SARAH3 satellite dataset was chosen, as recommended by the PVGIS manual for applications in South America (Joint Research Centre, 2024). The meteorological data from all databases were retrieved using the IO Tools functions available in the pvlib-python library (Jensen et al., 2023).

The decomposition models considered in the combinatory analysis included Disc (1987), Dirint (1992), Erbs (1966), and Boland (2001), as well as the direct and diffuse components provided directly by the selected SBD from the framework's stage of GHI analysis. The Perez (1990) transposition model was selected to compose the model chain, due to its widespread use in commercial PV modeling software and its proven reliability in predicting irradiance (Mahmoud et al., 2024; De Medeiros et al., 2025; PVsyst 8.0, 2025). The combination of DNI/DHI models that yielded the most accurate POA irradiance estimation, together with the chosen transposition model, was then used to build the final AC energy yield model chain.

All modeling procedures were implemented using pvlib-python version 0.13.1 (Holmgren et al., 2018), which provides validated and widely adopted physical models, consistent with those implemented in commercial PV simulation tools such as PVsyst 8.0 (2025). The physical model chain developed in this study is illustrated in Figure 2.

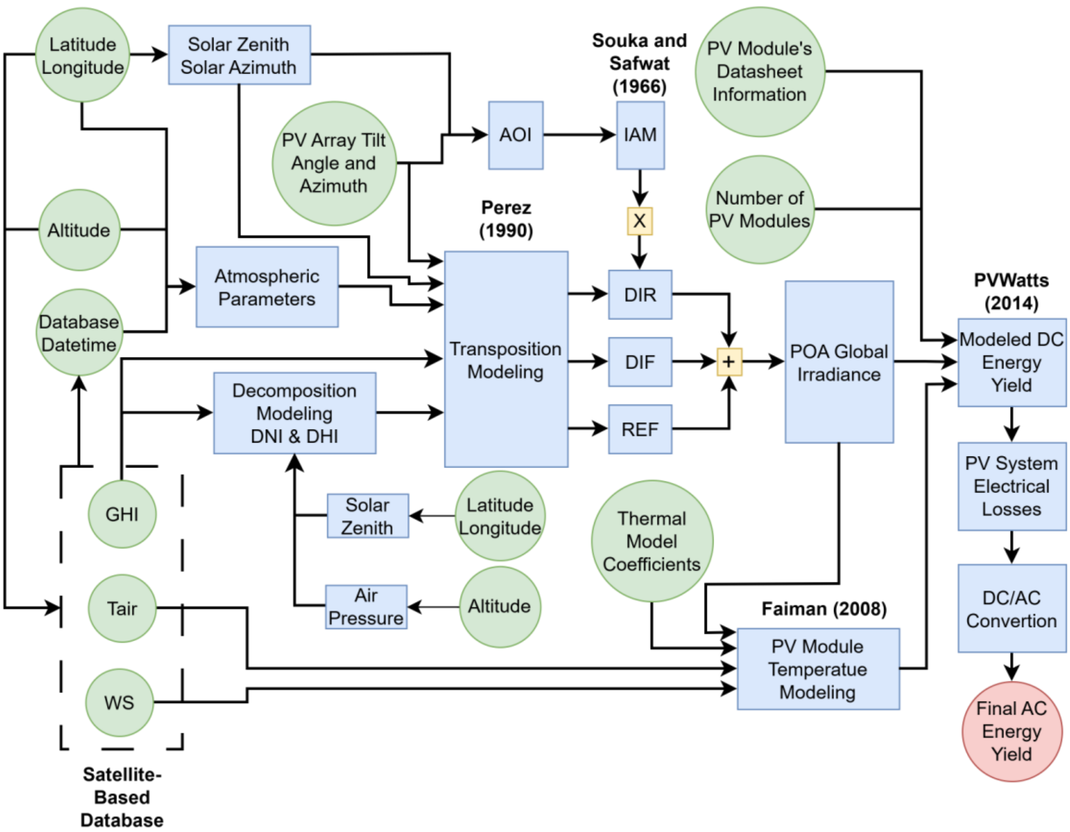

Figure 2: Flowchart of the proposed PV energy yield model chain.

In addition to the models defined for irradiance transposition, IAM losses, PV module temperature, and system power generation, standard pvlib-python models were adopted for determining atmospheric and secondary meteorological parameters, solar position, extraterrestrial irradiance (E_0), inverter parameters, and related variables. The electrical losses associated with mismatch, system unavailability, light-induced degradation (LID, as this was the plant's first operational year), ohmic wiring, and others, were defined according to the default configuration recommended in the PVWatts (Dobos, 2014) manual and implemented through pvlib-python functions (Holmgren et al., 2018). Since the PV power plant did not exhibit significant self-shading or inverter clipping effects, these losses were not considered in the AC energy yield modeling procedures.

3.3. Statistical Metrics for Performance Evaluation for Simulations Results and PV Power Plants Operation

To evaluate the predictions performance from the steps of SBDs selection, best pair of decomposition models, the AC energy yield and the PV system performance, metrics such as percentage difference (PD), Normalized Root Mean Square Error (nRMSE), Mean Absolute Percentage Error (MAPE), Percentage Bias (PBIAS), and the coefficient of determination (R^2) were applied, as done in the works of Dazhi et al. (2018), Salazar et al. (2020), Barros et al. (2025), and Riise et al. (2024).

For performance evaluation of the PV system, the performance metric adopted was the Performance Ratio (PR), as presented in Eq. 3. E_{out} represents the total AC energy yield of the PV system, according to the time resolution, i. This metric is used mainly for monthly and annual time resolutions, as recommended by the standard IEC 61724-1:2021.

$$PR = \frac{E_{out,i}}{P_0 * \frac{G_i}{G_0}} \qquad \text{(eq. 3)}$$

4. Results and Discussion

4.1. Selection of the Satellite Database

For the first analysis is considered the hourly, daily, and monthly time resolutions. For hourly time resolution comparatives, data treatment and time shift alignment were done. The night shifts values of hourly GHI excluded for the comparative analysis, avoiding misreading of the prediction's evaluation due to zero values. Daily and monthly timescales don't provide zero values, being more easily to make comparatives. Table 2 shows the results of performance estimations of the GHI from the three SBDs chosen for the present study. For the comparative of monthly PD, Figure 3 shows results for each SBD.

Table 2: Performance results of GHI estimations from distinct satellite databases over the year.

<table>
<tr><th rowspan="2">Time Scales</th><th colspan="3">nRMSE</th><th colspan="3">MAPE</th></tr>
<tr><th>NASA POWER</th><th>NSRDB</th><th>PVGIS 5.3 (SARAH3)</th><th>NASA POWER</th><th>NSRDB</th><th>PVGIS 5.3 (SARAH3)</th></tr>
<tr><td>Hourly</td><td>18.3</td><td>19.5</td><td>21.5</td><td>12.6</td><td>13.5</td><td>13.5</td></tr>
<tr><td>Daily</td><td>6.9</td><td>6.8</td><td>7.5</td><td>4.8</td><td>5.1</td><td>5.0</td></tr>
<tr><td>Monthly</td><td>1.5</td><td>3.3</td><td>2.0</td><td>1.1</td><td>2.9</td><td>1.4</td></tr>
<tr><th rowspan="2">Time Scales</th><th colspan="3">R²</th><th colspan="3">PBIAS</th></tr>
<tr><th>NASA POWER</th><th>NSRDB</th><th>PVGIS 5.3 (SARAH3)</th><th>NASA POWER</th><th>NSRDB</th><th>PVGIS 5.3 (SARAH3)</th></tr>
<tr><td>Hourly</td><td>0.915</td><td>0.904</td><td>0.883</td><td rowspan="3">-0.8</td><td rowspan="3">2.9</td><td rowspan="3">1.4</td></tr>
<tr><td>Daily</td><td>0.946</td><td>0.948</td><td>0.937</td></tr>
<tr><td>Monthly</td><td>0.994</td><td>0.969</td><td>0.989</td></tr>
</table>

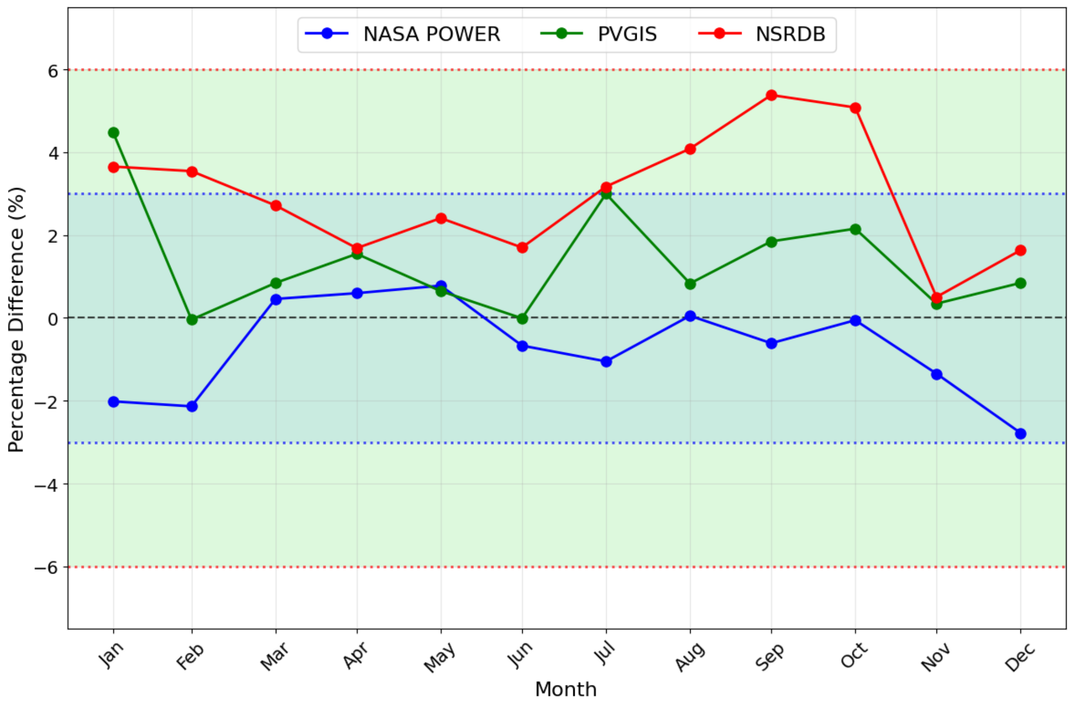

Figure 3: Monthly percentage difference between the modeled and measured GHI monthly values.

According to the results on Table 2 and on Figure 3, the NASA POWER database provided the most accurate and precise predictions of GHI under all-time scales and metrics, except of nRMSE and R^2 metrics under daily estimations which NSRDB provided slightly more accurate results. However, in general, the NASA POWER database outperformed the other two SBDs in terms of GHI estimations.

From Figure 3, all monthly GHI values from NSRDB are overestimated, in comparison with the monthly reference. Except for two months (February and June), PVGIS provided overestimated results as well. Meanwhile, the NASA POWER provided a negative annual bias due to the underestimated estimations of monthly GHI, in general, providing a slightly more conservative value of annual GHI, being necessary to be considered for further analysis of other steps of the proposed framework.

4.2. Combinatory Analysis for Chosen the Most Suitable Combination of DNI and DHI Components for POA Irradiance Modeling

The next step is to model the DNI/DHI components from NASA POWER GHI data and search for the pair of DNI/DHI sources which provide the most accurate results for POA global irradiance. After modeling the decomposed components of GHI and inputting 25 combinations of DNI/DHI based models and NASA POWER database pairs to model the POA global irradiance and comparing with the reference, Table 3 provides the top five ranking monthly results of the combinations.

Table 3: Top 5 ranking of decomposed components of NASA POWER'S GHI data, on monthly resolution.

Ranking	DNI Model	DHI Model	nRMSE	MAPE	PBIAS	R^2
1	Dirint	Erbs	2.2	1.8	0.4 %	0.983
2	Dirint	Boland	3.8	3.5	3.3	0.956
3	Disc	Erbs	4.5	3.6	3.3	0.939
4	Dirint	Disc	6.3	5.8	5.8	0.880
5	Disc	Boland	6.6	6.2	6.2	0.867

According to Table 3, the combination of decomposition models which contributed to the modeling of the most accurate monthly POA global irradiation among the rest of the possible combinations was for Dirint (DNI) and Erbs (DHI) models. The DNI and DHI estimations from SBD were outside the top ranking, becoming an important note about the necessity of exploration of different decomposition models to provide more accurate predictions of POA global irradiation. Figure 4 presents the monthly PD between the modeled and measured monthly summations.

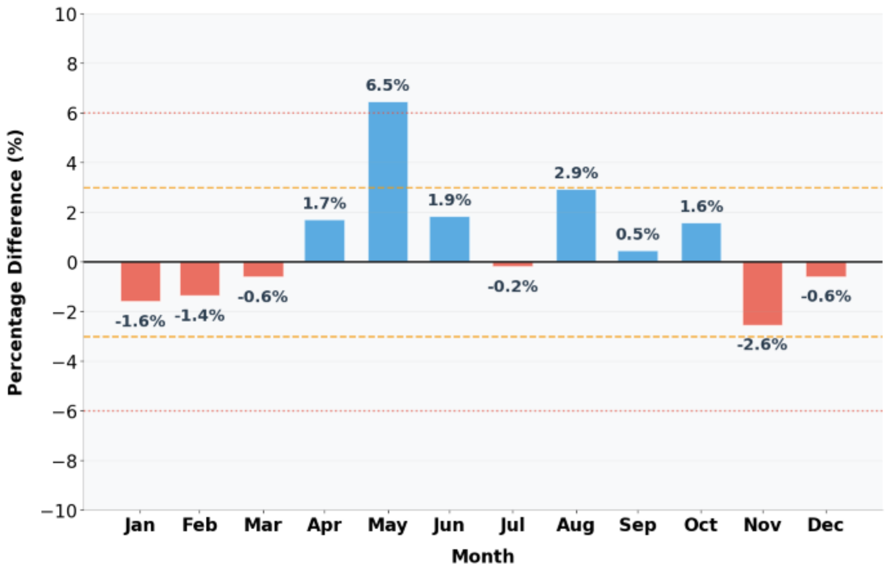

Figure 4: Monthly percentage difference from POA global irradiance modeled and measured.

In basis of the Figure 4, a pattern can be noted, which is that for summer months (December, January and February), the transition months between seasons (March, beginning of the fall season, and November, last month of the spring season), in addition of July month, the predictions were underestimated, meanwhile the months from April to October, except for July, showed overestimated results. Except for May (6.5%), all the months provided a PD lower than 3%. The nature of the results behavior is influenced by the seasonal weather conditions, cloud behavior, and other kinds of uncertainties such as measurements of the sensor, GHI estimations of chosen SBD, and decomposed components modeling, which can be deeper investigated for future works.

Calculating the POA global irradiation throughout the year, alongside SBD's air temperature and wind speed data and the thermal coefficients for Faiman model, the PV module temperature was calculated. As the PV module temperature measurements were not reliable enough, this parameter was not included in the present study, becoming an opening for future works to focus on reliable measurements of this parameter to improve the proposed framework.

4.3. AC Energy Yield Comparatives

From the modelled POA global irradiance and PV module's temperature, is possible to simulate the final AC energy yield of the system, considering the PV system losses and PV inverter efficiency from the model chain of the Figure 2. The performance metrics results of AC energy yield predictions for each PV inverter over the year are provided by Table 4.

Table 4: Performance evaluation metrics of AC energy yield predictions.

Performance Metrics	Inverter 1	Inverter 2	Inverter 3	Inverter 4	Inverter 5	Inverter 6
nRMSE (%)	5.48	6.60	5.35	3.97	3.06	3.23
MAPE (%)	4.38	5.01	4.69	2.86	2.42	2.62
PBIAS (%)	-1.15	0.15	-1.18	0.75	0.55	-0.44
R^2	0.901	0.887	0.891	0.942	0.965	0.963

According to Table 4, the modelled AC energy yield provided more accurate results for PV inverters 4 to 6 than the first three PV inverters for monthly results, despite the annual deviation (PBIAS) were lower than absolute 1.2% for all PV inverters. This kind of result needs attention, because having high accuracy on annual predictions does not indicates higher accuracy for monthly results. For instance, the PV inverter 2 provided the lowest annual bias deviation (+ 0.15%), but the highest values of nRMSE (6.6%), MAPE (5.01 %), and lower R^2 (0.887) among all PV inverters of the case study, indicating the most accurate annual predictions but the lowest accuracy on monthly scale.

4.4. Performance Ratio Comparatives

With the POA global irradiation and AC energy yield of the PV system modelled, the final stage of the proposed framework is the performance analysis through the PR index. In this stage, the monthly and annual PR estimates are evaluated under three different scenarios: 1) AC Energy Yield and POA global irradiation, both measured; 2) Measured AC Energy Yield and Modelled POA global irradiation; and 3) Modelled AC Energy Yield and Modelled POA global irradiation. Each scenario has a specific contribution for the analysis.

The first result represents the performance evaluation of PV power plant under operation, i.e., the measured PR, which is used as reference. The second scenario represents the performance evaluation of the PV system with the modelled POA global irradiation from the proposed framework, which is used to evaluate the accuracy of using the synthetic POA global irradiance and how far is it from the monthly and annual performance results of the reference. In the third scenario, the objective is to check the simulation of feasibility study, when there is no information about the AC energy yield. The Figure 5 shows the PR results under three scenarios over the six PV inverters, throughout the months of the year analysed.

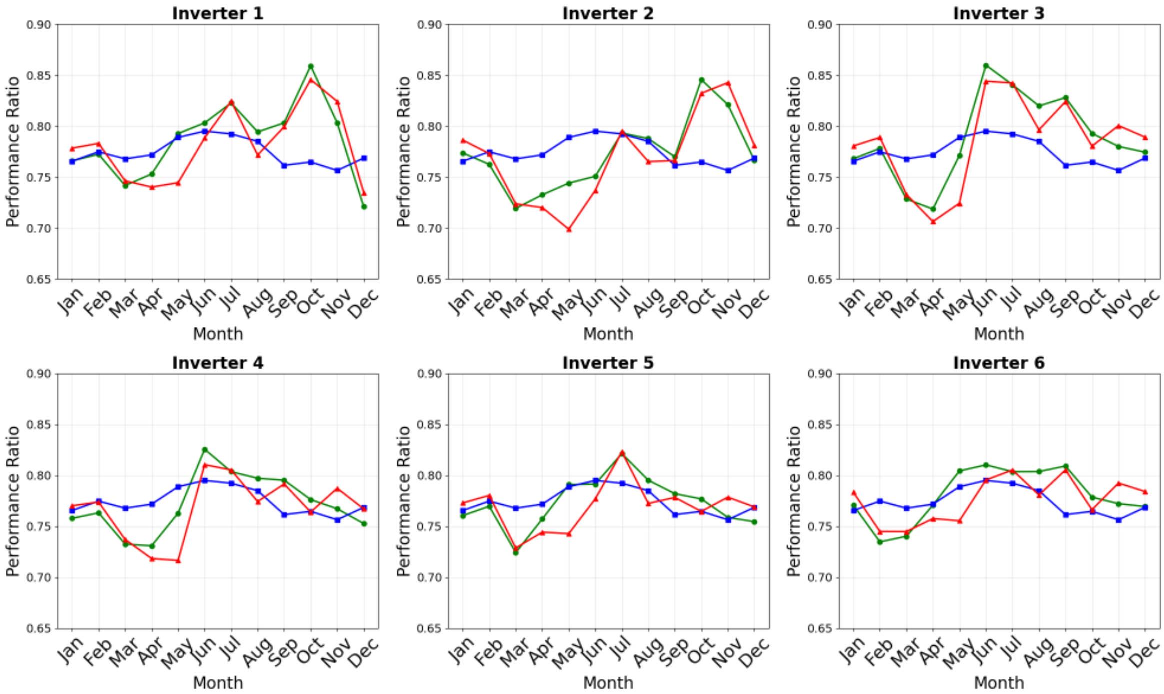

Figure 5: Performance Ratio estimation for six PV inverters from PV power plant in three scenarios: 1) Measured AC Energy and Measured POA Irradiance (Green); 2) Measured AC Energy and Modeled POA Irradiance (Red); and 3) Modeled AC Energy and Modeled POA (Blue).

According to Figure 5, the difference between modeled and measured monthly POA global irradiation directly affects the deviation of the monthly PR between the first and second scenarios. When POA irradiation is overestimated, the estimated PR decreases, whereas underestimation leads to higher PR values. This inverse relationship occurs because POA irradiation appears in the denominator of Eq. (3), indicating that the system seems less efficient when irradiation increases without a proportional rise in energy yield. The largest deviations were observed in May (6.5%) and August (2.9%), where the divergence between modeled and measured PR was most evident.

The third scenario does not alter inverter performance results, as it considers only modeled AC energy yield and POA global irradiation. Although this configuration presents visually higher monthly deviations compared to the reference scenario, its impact on annual predictions may differ. Table 5 summarizes the percentage-point discrepancies between the annual PR estimates for the second and third scenarios.

Table 5: Performance evaluation metrics of PR predictions.

PR Scenarios	Inverter 1	Inverter 2	Inverter 3	Inverter 4	Inverter 5	Inverter 6
Scenario 2	-0.0022 %					
Scenario 3	-0.0112 %	-0.001 %	-0.0114 %	0.0036 %	0.0020 %	-0.0056 %

According to Table 5, the second scenario underestimates the PR due to higher annual POA irradiation values. In contrast, although the third scenario shows larger monthly deviations from the reference case (Figure 5), the annual PR estimates derived from both modeled energy yield and POA irradiation differ by less than 0.012 percentage points for all PV inverters. These results demonstrate that the fully modeled approach remains suitable for annual performance evaluation and feasibility studies, confirming the robustness of the proposed model chain.

5. Conclusions

This study proposed a comprehensive and reproducible framework for evaluating the performance of PV power plants using a reduced number of sensors compared to those recommended by international standards. The framework comprises three main stages. The first involves selecting the SBD that provides the most accurate GHI data across different temporal resolutions. The second stage determines the optimal pair of decomposition models for accurately estimating POA irradiance. Finally, the third stage compares the modeled AC energy yield, obtained from the proposed model chain, with measured PV system performance under two scenarios, performance assessment and feasibility analysis, using the PR as the primary evaluation metric.

The framework was implemented in the pvlib-python environment and employed open-access SBDs, including NASA POWER, NSRDB, and PVGIS 5.3 (SARAH3), as meteorological inputs. Validation was performed using data from six monofacial single axis tracking PV power plants (3.74 MWp each) located in southeastern Brazil. Reference meteorological measurements were obtained from an IEC 61724-1:2021-compliant setup, consisting of three sensors at the solarimetric station and two sensors positioned at the module plane.

Results showed that the NASA POWER dataset provided the highest accuracy for GHI estimation and was therefore adopted for subsequent modeling steps. The combination of the Dirint model (for DNI) and the Erbs model (for DHI) yielded the most accurate monthly POA irradiance estimates, with deviations generally below 3%, except in May (up to 6.5%). The modeled monthly AC energy yield, when compared with inverter measurements across all PV plants, achieved nRMSE values between 3.05% and 6.6%, MAPE ranging from 2.42% to 5.01%, and annual bias below 1.2%. The modeled PR also showed strong agreement with field data, differing by less than 0.012 in absolute terms on an annual basis.

Overall, the proposed framework proved accurate and reliable for predicting solar resource and PV performance using only two strategically placed irradiance sensors, instead of the five recommended by standards. By relying solely on open-access datasets and free modeling tools, it offers a practical and cost-effective alternative for PV performance assessment. Future work should extend the framework with additional satellite databases, modeling options, uncertainties and error propagations due to the physical models from model chain, and data quality control procedures.

6. Acknowledgments

De Paula, J. F. et al. thanks TotalEnergies for the financial support. In addition, we are grateful to all collaborators from Universidade Estadual de Campinas (UNICAMP). Acknowledgements are extended to School of Electrical and Computer Engineering (FEEC). The work of G. Fraidenraich was supported by the Conselho Nacional de Desenvolvimento Científico e Tecnológico (CNPq) under Grant 302077/20227.

7. References

ABSOLAR, 2025. Infográfico. Disponível em: https://www.absolar.org.br [Acesso em: 17 outubro 2025].

Barros, I., Silva, J., Fernandes, A., Barros, T., Fantinato, D., Fraidenraich, G., 2025. Comparative analysis of spatial techniques for global horizontal solar irradiance estimation in the Brazilian context. 53rd Photovoltaic Specialists Conference (PVSC 2025).

Boland, J., Scott, L., Luther, M., 2001. Modelling the diffuse fraction of global solar radiation on a horizontal surface. Environmetrics 12(2), 103–116. https://doi.org/10.1002/1099-095X(200103)12:2%3C103::AID-ENV447%3E3.0.CO;2-2

BS EN IEC 61724-1, 2021. Photovoltaic system performance — Part 1: Monitoring. London: BSI Standards Publication.

BS ISO 9060, 2018. Solar energy — Specification and classification of instruments for measuring hemispherical solar and direct solar radiation. London: BSI Standards Publication.

Campos, R. A., Braga, M., Pires, A. M., Hohmann, M., Ovaitt, S., Rüther, R., 2025. Comparative analysis of rear irradiance modeling methods for bifacial PV systems on single-axis trackers under varying albedo conditions. Solar Energy 302, 114007. https://doi.org/10.1016/j.solener.2025.114007

Dazhi, Y., 2018. A correct validation of the National Solar Radiation Data Base (NSRDB). Renew. Sustain. Energy Rev. 97, 152–155. https://doi.org/10.1016/j.rser.2018.08.023

De Medeiros, J.V.F.F., Gomes, E.T.A., Alonso-Suárez, R., de Castro Vilela, O., 2025. Combining physical models to estimate PV power: Evaluation and optimal modeling in the solar resource-rich semi-arid Brazilian region. Renew. Energy 256, 123999. https://doi.org/10.1016/j.renene.2025.123999

De Paula, J.F.S., de Souza Silva, J.L., Barnabé, J.P.C., Campos, M.V., Dos Santos Barros, T.A., Fraidenraich, G., 2024. Comparative analyzes of parameters extraction models for photovoltaic modules using single diode model. 2024 16th Seminar on Power Electronics and Control (SEPOC), Santa Maria, Brazil, pp. 1-6. http://dx.doi.org/10.1109/SEPOC63090.2024.10747441.

Dobos, A.P., 2014. PVWatts version 5 manual. National Renewable Energy Laboratory (NREL), Golden, CO. Disponível em: http://pvwatts.nrel.gov/downloads/pvwattsv5.pdf [Acesso em: 17 outubro 2025].

Erbs, D.G., Klein, S.A., Duffie, J.A., 1982. Estimation of the diffuse radiation fraction for hourly, daily and monthly-average global radiation. Sol. Energy 28(4), 293–302.

Faiman, D., 2008. Assessing the outdoor operating temperature of photovoltaic modules. Prog. Photovolt: Res. Appl. 16(4), 307–315. https://doi.org/10.1002/pip.813

Holmgren, W., Hansen, C., Mikofski, M., 2018. pvlib python: a Python package for modeling solar energy systems. J. Open Source Softw. 3(29), 884. https://doi.org/10.21105/joss.00884

Jensen, A., Anderson, K., Holmgren, W., Mikofski, M., Hansen, C., Boeman, L., Loonen, R., 2023. pvlib iotools — Open-source Python functions for seamless access to solar irradiance data. Sol. Energy 266, 112092. https://doi.org/10.1016/j.solener.2023.112092

Jensen, A.R., Sifnaios, I., Anderson, K.S., Gueymard, C.A., 2025. SolarStations.org—A global catalog of solar irradiance monitoring stations. Sol. Energy 295, 113457. https://doi.org/10.1016/j.solener.2025.113457

Joint Research Centre, 2024. PVGIS: Photovoltaic Geographical Information System. Available at: https://joint-research-centre.ec.europa.eu/pvgis_en (accessed 4 May 2025).

Larrañeta, M., Fernandez-Peruchena, C., Silva-Pérez, M.A., Lillo-Bravo, I., Grantham, A., Boland, J., 2019. Generation of synthetic solar datasets for risk analysis. *Solar Energy* 187, 212–225. https://doi.org/10.1016/j.solener.2019.05.042

Liu, B. Y. H., Jordan, R. C., 1960. The interrelationship and characteristic distribution of direct, diffuse and total solar radiation. Solar Energy, [S.l.], v. 4, p. 1-19.

Mahmoudi, E., Silva, J.L.S., Barros, T.A.S., 2024. Assessing the performance of physical transposition models in photovoltaic power forecasting: A comprehensive micro and macro accuracy analysis. Energy Conversion and Management: X 24, 100792. https://doi.org/10.1016/j.ecmx.2024.100792

Masson, G., Bosch, E., Van Rechem, A., de l'Epine, M., 2024. Snapshot of Global PV Markets. IEA PVPS Task 1. https://doi.org/10.69766/VHRF4040

Maxwell, E.L., 1987. A quasi-physical model for converting hourly global horizontal to direct normal insolation. SERI/TR-215-3087, Solar Energy Research Institute, Golden, CO.

Meteonorm, 2025. Meteorological database. Disponível em: https://meteornom.com [Accessed in: 17 october 2025].

NASA Langley Research Center (LaRC) POWER Project. (2025). *Prediction Of Worldwide Energy Resources (POWER)*. National Aeronautics and Space Administration (NASA). Available at: https://power.larc.nasa.gov/ (Accessed: 17 October 2025).

National Renewable Energy Laboratory (NREL), 2025. National Solar Radiation Database (NSRDB). Disponível em: https://nsrdb.nrel.gov/ [Accessed in: 17 october 2025].

Perez, R., Ineichen, P., Maxwell, E., Seals, R., Zelenka, A., 1992. Dynamic global-to-direct irradiance conversion models. ASHRAE Trans. Res. Ser., 354–369.

Perez, R., Ineichen, P., Seals, R., Michalsky, J., Stewart, R., 1990. Modeling daylight availability and irradiance components from direct and global irradiance. Sol. Energy 44(5), 271–289.

PVsyst SA, 2025. PVsyst 8.0 Help. Disponível em: https://www.pvsyst.com/help/index.html [Acesso em: 17 outubro 2025].

Riise, H.N., Nygård, M.M., Aarseth, B.L., Dobler, A., Berge, E., 2024. Benchmark of estimated solar irradiance data at high latitude locations. Sol. Energy 282, 112975. https://doi.org/10.1016/j.solener.2024.112975

Salazar, G., Gueymard, C., Galdino, J.B., Vilela, O.C., Fraidenraich, N., 2020. Solar irradiance time series derived from high-quality measurements, satellite-based models, and reanalyses at a near-equatorial site in Brazil. Renew. Sust. Energ. Rev. 117, 109478. https://doi.org/10.1016/j.rser.2019.109478

Sengupta, M., Habte, A., Wilbert, S., Gueymard, C., Remund, J., Lorenz, E., van Sark, W., Jensen, A.R., 2024. Best practices handbook for the collection and use of solar resource data for solar energy applications, fourth ed. IEA PVPS. https://doi.org/10.69766/ENEH5295

Sengupta, M., Xie, Y., Zhang, J., Habte, A., Xiong, Y., 2025. Improving the National Solar Radiation Data Base using PSM V4. 53rd IEEE Photovoltaic Specialists Conference (PVSC), Montreal, Canada, pp. 1485–1487. https://doi.org/10.1109/PVSC59419.2025.11133215

SolarGIS, 2025. Solar resource data services. Disponível em: https://solargis.com [Acesso em: 17 outubro 2025].

Souka, A.F., Safwat, H.H., 1966. Determination of the optimum orientations for the double exposure flat-plate collector and its reflections. Sol. Energy 10, 170–174.

Wald, L., 2021. Fundamentals of solar radiation, first ed. CRC Press, Boca Raton. https://doi.org/10.1201/9781003155454

Yang, J., Sengupta, M., Bailey, M., Nychka, D., Habte, A., Bandyopadhyay, S., Xie, Y., 2024. Bias correction and statistical downscaling of future solar irradiance projections using the NSRDB. In: *Proceedings of the 2024 IEEE 52nd Photovoltaic Specialists Conference (PVSC)*. IEEE, USA. https://doi.org/10.1109/PVSC57443.2024.10748789